J. Biochem. 122, 918-926 (1997)

Overexpression in *Escherichia coli* of Chemically Synthesized Gene for Active 0.19 α-Amylase Inhibitor from Wheat Kernel[1]

Masahiko Okuda,[2] Takanori Satoh, Nobuhiko Sakurai,[3] Kazunori Shibuya,[4] Hiroyuki Kaji,[5] and Tatsuya Samejima[6]

Department of Chemistry, College of Science and Engineering, Aoyama Gakuin University, Chitosedai, Setagaya-ku, Tokyo 157

Received for publication, May 7, 1997

A synthetic gene encoding 0.19 α-amylase inhibitor (α-AI) from wheat kernel was obtained by enzymatic assembly of 18 oligodeoxynucleotides which were chemically synthesized. The synthetic gene was introduced into vector pET15b for expression in *Escherichia coli* BL21(DE3) under the control of T7 promoter. However, in SDS-PAGE and Western blotting analyses of the *E. coli* cell lysate, the expression product could not be detected. Expression analysis for various partially deleted gene fragments suggested that the putative hairpin-like structure of mRNA in the 5′-terminal coding region might interrupt efficient expression. When the hairpin structure was eliminated by using degenerate codons, the resulting gene could be overexpressed in *E. coli*. Although the gene product was accumulated in an insoluble fraction as inclusion bodies, its inhibitory activity could be recovered by solubilization with 8 M urea, followed by refolding through two successive steps of dialysis at alkaline pH. After purification, the recombinant 0.19 α-AI showed the same characteristics as the authentic inhibitor in terms of N-terminal amino acid sequence, peptide mapping on reverse-phase HPLC, far-UV circular dichroism (CD) spectrum and have inhibition of human salivary α-amylase. Thus, we have established an overexpression system in *E. coli* for active recombinant 0.19 α-AI.

Key words: α-amylase inhibitor, hairpin structure, recombinant, synthetic gene, wheat kernel.

Proteinous α-amylase inhibitors (α-AIs) are widespread in microorganisms (*Streptomyces*) (*1-7*) and higher plants, and specifically inhibit α-amylases. Relatively small α-AI molecules from microorganisms have been intensively studied. In particular, the three-dimensional structures of Tendamistat (HOE467) from *S. tendae* 4158 and Haim I from *S. griseosporeus* YM-25 have been determined by NMR spectroscopy or X-ray crystallography and from these results the putative active sites have been identified (*8-10*). Also, the three-dimensional structures of mutant Tendamistat (*11*) and Tendamistat-porcine pancreatic α-amylase complex (*12*) have been determined and the inhibitory mechanisms have been analyzed at the molecular level. On the other hand, plant α-AIs have been isolated from wheat kernel, barley (*13*), rye (*14*), kidney bean (*15*), and other plants (*16-18*), but they have not yet been investigated in detail. However, the three-dimensional structures of the bifunctional α-amylase/proteinase K inhibitor from wheat (*19*) and α-amylase/trypsin inhibitor from ragi (*20*) have been determined recently.

A variety of α-AIs occur in the wheat kernel (*21*) and they can be classified into endogenous and exogenous α-AIs. The endogenous α-AIs inhibit α-amylases from plants and microorganisms, but can not inhibit mammalian and insect enzymes. In contrast, the exogenous α-AIs inhibit mammalian and insect α-amylases, while they have no inhibitory activity towards the enzymes from plants and microorganisms. Furthermore, the exogenous α-AIs can be grouped into three families of 60,000, 26,000, and 13,000 Da according to their molecular mass (*21*). Among them, 0.19 (*22*), 0.28 (*23*), and 0.53 α-AIs (*24*), distinguished by their relative gel electrophoretic mobility, have so far been studied in detail (*25-28*). The 0.19 α-AI belonging to the 26,000 family consists of two identical subunits, each composed of 124 amino acids, and is assumed to have five intrachain disulfide bonds. The inhibitor forms a 1:1 complex with the amylase and can inhibit human salivary α-amylase ninetyfold more effectively than human pancre-

[1] The nucleotide sequence in this paper has been submitted to DDBJ, Gene Bank, and EMBL nucleotide sequence databases with the accession number AB003682.

Present addresses: [2]Graduate School of Integrated Science, Yokohama City University, Seto, Kanazawa-ku, Yokohama, Kanagawa 236; [3]Division of Life Sciences, Graduate School of Natural Science and Technology, Kanazawa University, Kakumamachi, Kanazawa, Ishikawa 920-11; [4]Department of Molecular Biology, School of Medicine, Keio University, Shinanomachi, Shinjuku-ku, Tokyo 160; [5]Department of Chemistry, Faculty of Science, Tokyo Metropolitan University, Minami-osawa, Hachioji, Tokyo 192-03.

[6] To whom correspondence should be addressed. Tel: +81-3-5384-1111 (Ext. 3204), Fax: +81-3-5384-6200, E-mail: samejima@fatima.chem.aoyama.ac.jp

Abbreviations: α-AI, α-amylase inhibitor; ADK, porcine adenylate kinase; BCIP, 5-bromo-4-chloro-3-indolyl phosphate; CBB, Coomassie Brilliant Blue; HSA, human salivary α-amylase; IPTG, isopropyl-β-D-thiogalactopyranoside; NBT, nitro blue tetrazolium; RBI, bifunctional α-amylase/trypsin inhibitor from ragi seed.

atic α-amylase (*22*). The elucidation of the mechanism of the specific interaction between 0.19 α-AI and the target amylases is an intriguing problem from the viewpoint of molecular recognition. We had planned to identify the reactive amino acid residues in the molecule, and we conducted several chemical modifications, obtaining some significant data. This approach, however, seemed unlikely to permit any definitive conclusion. Therefore, to confirm our preliminary speculations on the reactive sites, we attempted to utilize site-directed mutagenesis. Although the 0.19 α-AI gene is known to be located in the short arm of chromosome 3D (*29*), it has not yet been cloned thus far. We tried to construct a synthetic 0.19 α-AI gene for the following three reasons: (1) the whole amino acid sequence has already been determined, (2) it is a relatively small protein, so construction of the gene seemed feasible, and (3) we could incorporate appropriate restriction enzyme recognition sites. In this paper, we describe the molecular cloning of a chemically synthesized gene for 0.19 α-AI, the development of an overexpression system in *Escherichia coli*, solubilization of the insoluble expression product, and refolding to an active form, as well as the characterization of the purified protein.

MATERIALS AND METHODS

Materials—*E. coli* strain JM109 and plasmid pUC118 used for cloning were obtained from Toyobo and Takara Shuzo, respectively. Plasmid pET15b and *E. coli* BL21-(DE3) for expression were purchased from Novagen. Restriction endonucleases and DNA-modifying enzymes were purchased from Nippon Gene. Alkaline phosphatase-conjugated goat anti-rabbit IgG and its substrates (5-bromo-4-chloro-3-indolyl phosphate [BCIP] and nitro blue tetrazolium [NBT]) used for immunoblotting were products of Promega Biotech. The chemicals used in this study were all of reagent grade. The authentic 0.19 α-AI was extracted from wheat flour and purified essentially according to the method of O'Connor and McGeeney (*30*) by ammonium sulfate fractionation (10-50% sat.), followed by 1st DEAE-Sephacel, QEA-Sephadex, and 2nd DEAE-Sephacel column chromatographies. The purity and mobility of the inhibitor were examined by electrophoretical analysis.

Synthesis of Oligodeoxyribonucleotides—The 18 single-stranded oligodeoxyribonucleotides (oligomers) to be assembled were synthesized by the solid-phase phosphoramidite method with an Applied Biosystems 381A DNA synthesizer according to the procedures recommended by the manufacturer. The synthesized oligomers were cleaved from the controlled pore glass with 2 ml of conc. NH_4OH solution, and deprotected at 55°C for 10 h, then NH_4OH was removed by the use of a rotary vacuum evaporator.

Design and Construction of the Synthetic Gene for 0.19 α-AI—The synthetic gene for 0.19 α-AI was designed to be composed of the coding region with tandem termination codons and a linker region, which was constructed from the 18 oligomers synthesized. The optimal codon usage for *E. coli* was employed and some restriction endonuclease recognition sites were introduced into the gene for convenience as shown in Fig. 1. The gene fragments encoding the N- and C-terminal halves (half position is the *Sph*I site around Met 60) of the inhibitor were constructed from eight and ten oligomers, respectively. Equimolar amounts of 5′-phosphorylated oligomers were mixed and then annealed by heating at 70°C for 10 min, followed by slow cooling to room temperature. The resulting N- and C-terminal fragments were ligated separately into the multiple cloning sites of pUC118. The N-terminal fragment was ligated into the *Eco*RI-*Sph*I sites of pUC118, and the C-terminal fragment was ligated into the *Sph*I-*Hin*dIII sites by T4 DNA ligase. The plasmids were named pUCAI-N and pUCAI-C, respectively. They were digested with *Sph*I and *Hin*dIII, and the C-terminal fragment from pUCAI-C was ligated into the *Sph*I-*Hin*dIII sites of pUCAI-N. The resulting plasmid including the full-length 0.19 α-AI gene was designated as pUCAI-I.

Construction of the Expression Vector for 0.19 α-AI—The strategy for construction of the expression vector is shown in Fig. 2. The cloning plasmid vector pUCAI-I was digested with *Hin*dIII and the generated sticky ends were filled with Klenow fragment (these filled-in restriction sites are illustrated by the symbol #), followed by *Nco*I digestion. The truncated 0.19 α-AI gene fragment was ligated into the *Nco*I-*Bam*HI# sites of pET15b, which was treated with *Bam*HI, Klenow fragment, and *Nco*I successively. The resulting plasmid vector was named pETAI-0. A fragment encoding the missing N-terminal region of α-AI was prepared from two oligomers, 5′-CATGTCTGGTCCATG-GATGTGCTACCC-3′ and 5′-GGGTAGCACATCCATGG-ACCAGA-3′. This fragment was then ligated into the *Nco*I-*Sma*I sites of pETAI-0, which was treated with the same restriction enzymes. The obtained expression vector for full-length 0.19 α-AI was designated as pETAI-I.

Expression of 0.19 α-AI Gene in E. coli—The expression plasmid vector pETAI-I was transformed into *E. coli* BL21(DE3). The transformant was cultured in 1.5 ml of LB-broth (1% Difco tryptone, 0.5% Difco yeast extract, and 1% NaCl) containing 100 μg/ml of ampicillin (LB/Amp) at 37°C. When the absorbance of the culture reached 0.6 at 660 nm, expression was induced by adding isopropyl-β-D-thiogalactopyranoside (IPTG) at the final concentration of 0.5 mM. After 3 h, aliquots of 0.2 ml of the culture were collected and centrifuged. The pellets were suspended in 32 μl of SDS-PAGE sample buffer (1.2% SDS, 12 mM Tris-Glycine, pH 6.8, 0.025% bromophenol blue, 1.5% 2-mercaptoethanol) and lysed by sonication. The lysate was boiled for 5 min and then subjected to SDS-PAGE and Western blotting.

SDS-PAGE and Western Blotting—SDS-PAGE was performed on 15% polyacrylamide slab gel under reducing conditions (*31*). The gel was stained with Coomassie Brilliant Blue (CBB) R-250. Following the electrophoresis, proteins were electroblotted onto a nitrocellulose membrane. The membrane was treated with masking solution (3% BSA in TS buffer, which is composed of 10 mM Tris-HCl at pH 8.0, 50 mM NaCl) for 30 min, and incubated with rabbit antiserum against 0.19 α-AI in masking solution for 30 min at room temperature. It was washed with 0.1% Tween 20 in TS buffer, then incubated with alkaline phosphatase-conjugated goat anti-rabbit IgG in TS buffer for 30 min and bands were visualized by using a ProtoBlot Immunoblotting system with NBT, and BCIP in AP solution (100 mM Tris-HCl, at pH 9.5, 150 mM NaCl).

Calculation of the Free Energy of mRNA Secondary Structure—The prediction of mRNA secondary structure

for 0.19 α-AI from the base sequence of the synthetic gene and the calculation of the free energy of the predicted hairpin structure was performed by GENETYX programs (Software Development, Tokyo) (*32*). For the prediction, the matching percentage of stem parts was set at 63, and the maximum and minimum sizes of search for both stem and loop parts were set at 11 and 10. For the calculation, the minimum length of stacking region was set at 2.0 and the maximum stacking energy (kcal/mol) was set at −10.

Expression Efficiency Analysis for the Deleted Genes—Deletion analysis was carried out in the fusion protein expression system of porcine adenylate kinase (ADK) and 0.19 α-AI, since the ADK gene had been confirmed by expression downstream of the *tac* promoter on the expression vector pMAXC in *E. coli* (*33*). The 0.19 α-AI gene was deleted after a consideration of hairpin structures of mRNA detected by the GENETYX programs and ligated into the midstream of the ADK gene, in-frame. A plasmid including the fused gene of ADK and the full-length 0.19 α-AI was designated as pAAf-1 and constructed as follows. The pMAXC was digested with *Afl*II and the sticky ends were filled with Klenow fragment (*Afl*II#), then digested with *Hin*dIII. The pUCAI was digested with *Eco*RI, filled with Klenow fragment (*Eco*RI#), and then digested with *Hin*dIII. Ligation of the 0.19 α-AI gene fragment (*Eco*RI#-*Hin*dIII) into the *Afl*II#-*Hin*dIII sites of pMAXC generated pAAf-1. Three plasmids including the fused genes of ADK and truncated 0.19 α-AI were named pAAf-D1, pAAf-D2, pAAf-D3 and constructed, respectively, as follows: the pMAXC and pUCAI were digested with *pvu*II and *Hin*dIII. Ligation of the 0.19 α-AI gene fragment (*pvu*II-*Hin*dIII) from pUCAI into the *pvu*II-*Hin*dIII sites of pMAXC yielded pAAf-D1. For pAAf-D2, pMAXC was digested with *Sma*I and *Hin*dIII, while pUCAI was digested with *Nae*I and *Hin*dIII. Ligation of the 0.19 α-AI gene fragment (*Nae*I-*Hin*dIII) into the *Sma*I-*Hin*dIII sites of pMAXC generated pAAf-D2. To obtain pAAf-D3, pMAXC and pUCAI were digested with *Sma*I and *Hin*dIII. Ligation of the 0.19 α-AI gene fragment (*Sma*I-*Hin*dIII) into the *Sma*I-*Hin*dIII sites of pMAXC resulted in pAAf-D3. The gene products were detected by SDS-PAGE.

Modification of the 5′-Terminal Region of the 0.19 α-AI Gene—The codon usage for the N-terminal region of the 0.19 α-AI gene was changed by the PCR technique on an ATTO Zymoreactor model II AB-1820 with an improved primer 5′-ACGAATTCATGAGTGGTCCATGGATGTGT-TACCCAGGTCAAGCATTCC-3′ as the sense primer and the oligomer, 5′-CTGCGCGCCGTGTTCTTTGTACATA-GAGTCCAGCATG-3′ used in the construction of the 0.19 α-AI gene, as the antisense primer. The resulting PCR product was cloned into vector pUCAI-I after digestion with *Eco*RI and *Sph*I. This exchange of N-terminal fragment generated the cloning vector pUCAI-II including the modified 0.19 α-AI gene. The modified expression vector, pETAI-II was constructed by exchanging the *Nco*I-*Nsi*I fragment from pETAI-I for the one from pUCAI-II.

Renaturation and Purification of Recombinant 0.19 α-AI—*E. coli* BL21(DE3) transformed with pETAI-II was cultured in 1 liter of LB/Amp at 37°C. After cultivation for 3 h in the presence of 0.5 mM IPTG, the culture was held for 30 min on ice and cells were harvested by centrifugation at 6,000 rpm for 30 min. The pellets were suspended in water and the cells were harvested by centrifugation at 6,000 rpm for 15 min. The pellets were resuspended in 10 mM Tris-HCl, pH 8.0 and sonicated five times for 1 min each. The insoluble fraction was collected by centrifugation at 6,000 rpm for 15 min and dissolved in 8.0 M urea in 10 mM Tris-HCl, pH 8.0, followed by incubation for 30 min at 37°C. After centrifugation, the supernatant was collected and diluted tenfold with the same solution. The diluted solution was dialyzed against 50 mM Tris-HCl, pH 10.0 for 6–16 h at room temperature and then against 50 mM Tris-HCl, pH 9.0 for 16 h. Insoluble matter precipitated during the dialysis was removed by centrifugation and the supernatant was loaded on a DEAE-Sephacel column equilibrated with 50 mM Tris-HCl, pH 9.0. After having been washed with the same buffer, proteins were eluted with a linear gradient of 0–150 mM NaCl in the same buffer. The fractions containing inhibitory activity were pooled and dialyzed against water for 16 h at room temperature, followed by lyophilization. The preparation was dissolved in 50 mM Tris-HCl, pH 9.0, and applied to a column of Shodex DEAE-825 (8.0 mm×75 mm). The conditions of equilibration and elution were the same as those described above. The protein in a single peak was pooled and used for the characterization of recombinant 0.19 α-AI after its purity had been confirmed by native PAGE.

Amino Acid Sequencing—After SDS-PAGE, proteins were electroblotted onto a polyvinylidene difluoride membrane (Immobilon-P; Millipore) and stained with CBB. The band corresponding to 0.19 α-AI on the membrane was cut out, and applied to an automated protein sequencer (Applied Biosystems 477A).

Peptide Mapping—The lyophilized recombinant and authentic 0.19 α-AIs were denatured in 500 mM Tris-HCl, pH 8.1, containing 6.0 M guanidine-HCl, 2.0 mM EDTA for 90 min at 50°C. They were reduced with 22 μM dithiothreitol for 4 h at 50°C, then carboxymethylated with 54 μM monoiodoacetic acid for 20 min at room temperature in the dark. The resulting reduced and carboxymethylated 0.19 α-AIs were dialyzed against 5.0 mM NH_4HCO_3 at pH 8.0 for 48 h at room temperature, and digested with V8 protease (*Staphylococcus aureus* protease) for 24 h at 37°C. The reaction was stopped with 1 N HCl and the resultant peptides were applied to a reverse-phase column of μ BONDASPHERE 5μC18-300 Å (3.9 mm×150 mm). The elution profiles were obtained with a linear gradient of 0–60% acetonitrile in 0.1% trifluoroacetic acid (TFA).

Circular Dichroism (CD) Spectra—CD spectra of the recombinant and authentic 0.19 α-AIs were measured with a Jasco J-600 CD dichrograph at room temperature. The scanning range was 250–190 nm and the path length of the quartz cell was 1.0 mm. The concentrations of 0.19 α-AIs were 0.10 mg/ml.

Measurement of Inhibitory Activity—Forty microliters of 35 μg/ml human salivary α-amylase (HSA), 40 μl of 1.25–10 μg/ml 0.19 α-AI, and 20 μl of 20 mM HEPES-NaOH, pH 7.0, containing 20 mM $CaCl_2$, were preincubated for 15 min at 37°C. Forty microliters of the reaction solution was added to 1.0 ml of 0.10% soluble starch solution, and the whole was incubated for 1 min at 37°C. To stop the reaction, 1.0 ml of I_2-KI solution (0.33% I_2, 3.3% KI) was added. After 5 min at room temperature, the reaction solution was diluted with 8.0 ml of water. After 15 min at room temperature, the absorbance at 660 nm was

measured. Remaining activity of HSA was measured using the following equation: Remaining activity of HSA(%) = $100 \times \Delta A_i / \Delta A$ where ΔA is the difference of absorbance between a reagent blank and inhibitor blank and ΔA_i is the difference of absorbance between a reagent blank and sample.

RESULTS AND DISCUSSION

Design and Construction of Chemically Synthesized Gene for 0.19 α-AI—We first cloned a gene for α-AI by artificial assembly of synthesized oligoDNA fragments. The synthetic gene for 0.19 α-AI was a 390 bp DNA fragment containing a coding region (125 amino acids, 375 bp), and two translation termination codons for complete termination (Fig. 1). We divided the whole gene into 18 oligomers, from 30 mer to 49 mer, and introduced 15 restriction endonuclease recognition sites into the gene to facilitate genetic manipulations. In the construction of the 0.19 α-AI gene, the N- and C-terminal fragments were prepared by annealing all the component oligomers simultaneously. Each subcloning vector, pUCAI-N or pUCAI-C, had an insertion of about 200 bp, and its sequence was verified by using a fluorescence DNA sequencer (Hitachi SQ-3000) (*34*). The gene segments encoding the N- and C-terminal halves were connected to construct the complete 0.19 α-AI gene (cloning vector pUCAI-I), and the sequence was confirmed by sequencing and restriction enzyme mapping (data not shown here).

Expression of 0.19 α-AI Gene in E. coli—To express the synthetic gene in *E. coli*, it was introduced downstream of the T7 promoter in plasmid vector pET15b (Fig. 2). The resulting expression vector pETAI-I was transformed into *E. coli* BL21(DE3) and the transformant was grown in LB/Amp medium at 37°C. After induction with 0.5 mM IPTG, the cells were subjected to SDS-PAGE and Western blot analysis. The expression product was not detected (Fig. 3, lane 2). The proteins in lanes 2 and 3 showed multiple bands on Western blotting, which may be due to non-specific binding of the antibody with these proteins. The authentic α-AI in lane 4 showed two bands, of which the upper band may be an oxidized form of α-AI. Although the SDS-PAGE for Western blotting was performed in the presence of β-mercaptoethanol, the reduced form may be partially oxidized (Fig. 3B). As a first step, we tested the efficiency of translational initiation (*35-37*). We prepared pAAf-I, a fused gene of 0.19 α-AI preceded by ADK, for which efficient translational initiation is assured owing to the overexpression in *E. coli*, and examined expression of the fusion protein. The result of SDS-PAGE showed that the translational initiation for the fused gene proceeded smoothly as expected, but a significantly smaller-than-expected fusion protein was produced (Fig. 4B, lane 2), its molecular mass being approximately 10-12 kDa in contrast with the predicted molecular mass of about 24 kDa for the fusion protein. This strongly suggested that the expression of the fusion gene was interrupted near the 5'-terminal region of the 0.19 α-AI gene. However, it was unclear

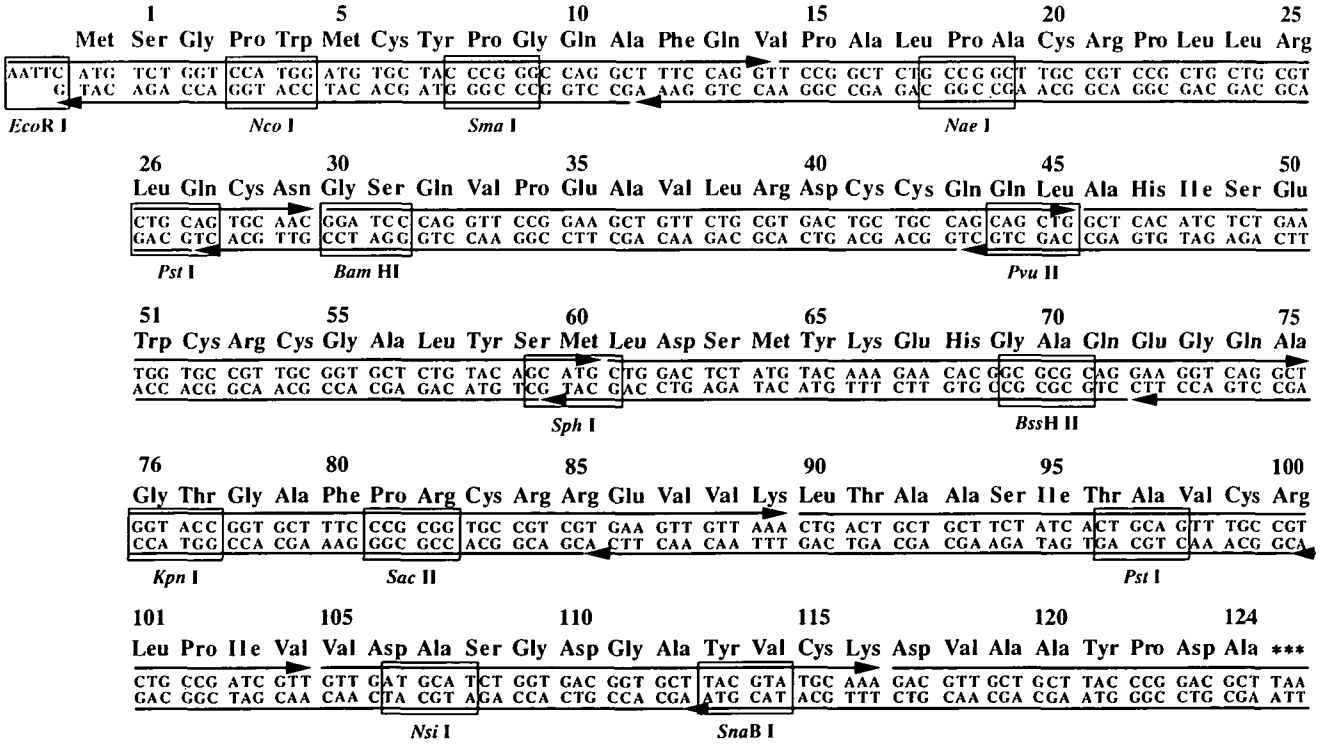

Fig. 1. **Design of synthetic gene for 0.19 α-AI.** The nucleotide sequence was designed with optimum codon usage of *E. coli* according to the amino acid sequence. The synthetic gene is composed of the coding region (125 amino acids, 375 base-pairs), two termination codons and a linker region for connection to the vector. The asterisks indicate translation termination codons. The arrows below or above the nucleotide sequence indicate the direction (5'→3') of individual single-stranded oligodeoxy-ribonucleotides synthesized. Restriction endonuclease recognition sites are boxed.

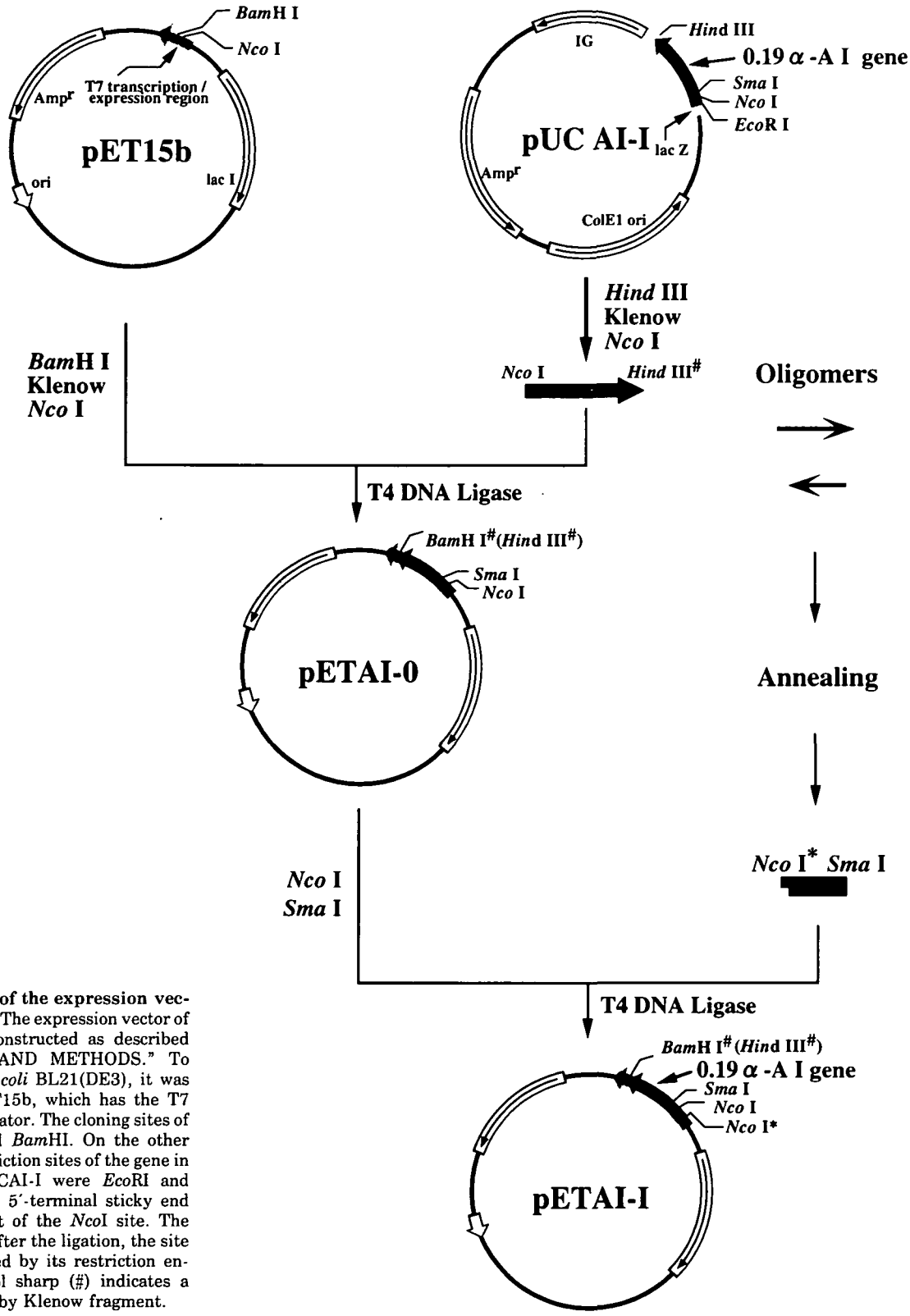

Fig. 2. **Construction of the expression vector for 0.19 α-AI gene.** The expression vector of 0.19 α-AI gene was constructed as described under "MATERIALS AND METHODS." To express the gene in *E. coli* BL21(DE3), it was ligated into vector pET15b, which has the T7 promoter and T7 terminator. The cloning sites of pET15b were *Nco*I and *Bam*HI. On the other hand, the terminal restriction sites of the gene in the cloning vector pUCAI-I were *Eco*RI and *Hin*dIII. Therefore, the 5′-terminal sticky end must be altered to that of the *Nco*I site. The asterisk indicates that after the ligation, the site was no longer recognized by its restriction endonuclease. The symbol sharp (#) indicates a restriction site filled-in by Klenow fragment.

whether the interruption occurred at the transcription or the translation step. To follow up this unexpected observation, we tried to identify the region responsible for the interruption by deleting various parts capable of forming a hairpin structure (Fig. 4). We predicted the secondary structures of mRNA by using the GENETYX program; eight hairpin structures were predicted, of which five were located near the N-terminal region of the inhibitor (Fig. 4). They were named H1-H8 in the order from the 5′-terminus. Moreover, the minimum free energy of each hairpin

structure was calculated (Table I). To examine whether hairpin structure of mRNA interrupts expression and if so, to identify which hairpin is predominantly responsible, we prepared three truncated 0.19 α-AI genes, named pAAf-D1, pAAf-D2, and pAAf-D3 (Fig. 4A). The expression efficiency was readily monitored by SDS-PAGE of the expression product. The SDS-PAGE profile showed that the molecular mass of the pAAf-D1 gene product coincided with the predicted value (Fig. 4B, lane 3). The expression products of pAAf-D2 deleting H1 and H2 also showed the predicted molecular masses (Fig. 4B, lane 4). The pAAf-D3 lacking H1 only produced a normal expression product (Fig. 4B, lane 5). Since the elimination of the most stable hairpin, H1 (−18.31 kcal/mol), led to adequate synthesis of full fusion protein, H1 was identified as the sole critical element preventing effective expression (Fig. 5).

Expression of an Improved 0.19 α-AI Gene in E. coli— To eliminate the putative hairpin structure H1, the 5′-terminal region was modified by PCR using an improved primer designed by taking advantage of degenerate codons. Destabilization by five substitutions (+21:C→U, +27:G→A, +30:C→U, +33:G→A, +36:U→A) in the expression vector pETAI-II was expected to increase the minimum free energy from −18.31 to −12.10 kcal/mol (Fig. 5). Thus, we constructed an improved gene with these nucleotide substitutions. To examine the expression of the improved gene in *E. coli*, pETAI-II was introduced into *E. coli* BL21(DE3) and the resultant transformant was cultivated. Aliquots of the cells were subjected to SDS-PAGE and Western blot analysis (Fig. 3). The SDS-PAGE showed a strong band with the same mobility as that of authentic 0.19 α-AI (Fig. 3A, lane 1) and this band was also detected by Western blot analysis (Fig. 3B, lane 1).

Thus, the five codon alterations to destabilize the H1 structure led to overexpression of the improved gene, and the destabilization was estimated as 6.21 kcal/mol. We also succeeded in obtaining overexpression with an expression vector pMKAI-II (*tac* promoter) in a synthetic two-cistron expression system (*38*) by the same method (data not shown). We are still not clear how the hairpin structure functions in *E. coli*, but our results suggest that the specific secondary structure in the mRNA influenced its expression.

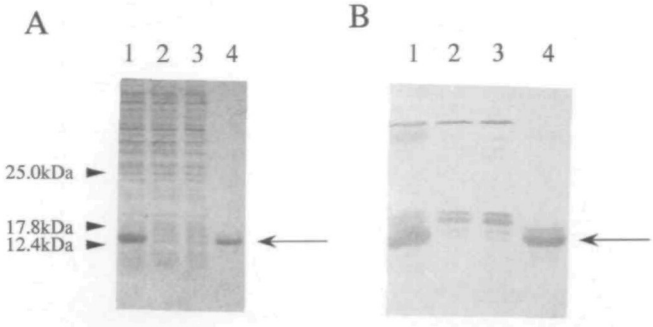

Fig. 3. **Expression of 0.19 α-AI gene in *E. coli*.** SDS-PAGE and Western blotting were performed as described under "MATERIALS AND METHODS." Panels A and B show SDS-PAGE and Western blotting, respectively, for identical samples. Lane 1, total cellular proteins derived from the expression vector pETAI-II; lane 2, pETAI-I transformant; lane 3, control vector pET15b transformant; lane 4, authentic 0.19 α-AI.

TABLE I. **Predicted hairpin structures of mRNA for 0.19 α-AI and their minimum free energy.**

Hairpin name	Minimum free energy (kcal/mol)	Sequence position[a]
H1	−18.31	3- 35
H2	−12.30	40- 72
H3	−13.61	65- 94
H4	−5.61	89-120
H5	−7.72	103-132
H6	−5.35	170-202
H7	−12.10	226-256
H8	−9.10	302-333

[a]Sequence begins at A of the translation initiation codon AUG.

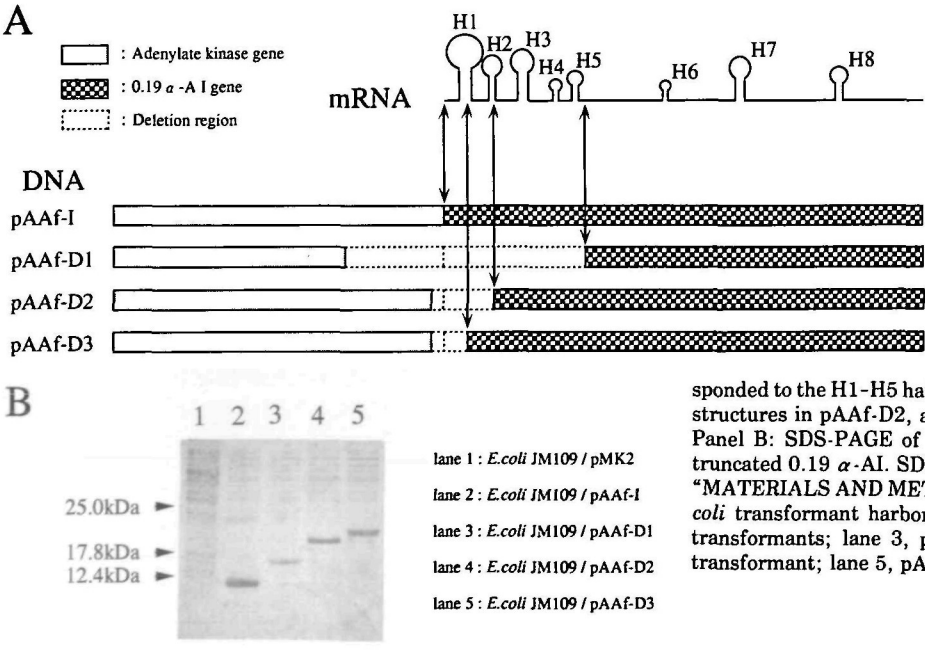

Fig. 4. **Deletion analysis.** Panel A: Predicted mRNA hairpin structures on 0.19 α-AI mRNA from its gene and the fused gene of ADK and the intact or truncated 0.19 α-AIs. The expression analysis for various deleted genes was performed as described under "MATERIALS AND METHODS." On the mRNA, ♀ represents a hairpin structure and its height indicates the stability of the mRNA molecule. For the gene DNA, the pAAf-I was composed of ADK gene and full-length 0.19 α-AI gene. For three deleted genes, the deleted region of 0.19 α-AI gene corresponded to the H1-H5 hairpin structures in pAAf-D1, H1-H2 hairpin structures in pAAf-D2, and only H1 hairpin structure in pAAf-D3. Panel B: SDS-PAGE of the fusion protein for ADK and intact or truncated 0.19 α-AI. SDS-PAGE was performed as described under "MATERIALS AND METHODS." Lane 1, total cellular protein of *E. coli* transformant harboring control vector pMK2; lane 2, pAAf-I transformants; lane 3, pAAf-D1 transformants; lane 4, pAAf-D2 transformant; lane 5, pAAf-D3 transformant.

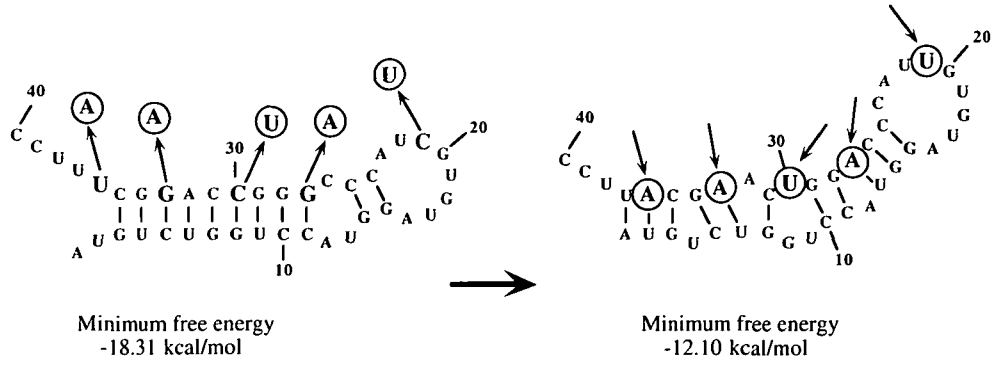

Fig. 5. **Improvement of 5′-terminal region in 0.19 α-AI gene.** The destabilization of H1 hairpin structure was achieved by base substitution. The prediction of mRNA secondary structure and the calculation of its minimum free energy were performed by using the GENETYX program as described under "MATERIALS AND METHODS." The numbers indicate positions in the base sequence from the beginning of the translation initiation codon. The substituted bases are enclosed with circles. Left: H1 hairpin structure. Right: destabilized H1 hairpin structure.

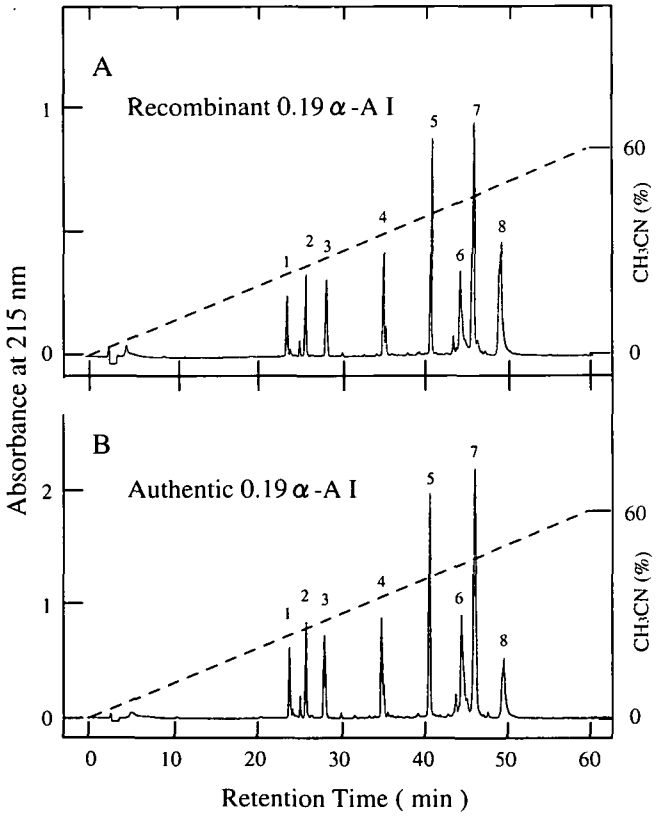

Fig. 6. **Comparison of peptide maps of recombinant and authentic 0.19 α-AI.** Both 0.19 α-AIs were carboxymethylated and digested as described under "MATERIALS AND METHODS." Panel A shows the elution profile of recombinant 0.19 α-AI and Panel B, that of authentic 0.19 α-AI. The elution profiles were obtained by using a reverse-phase column of μ BONDASPHERE 5μC18-300A (3.9 mm×150 mm) with a linear gradient of 0-60% acetonitrile solution. The main peaks are numbered according to the order of elution.

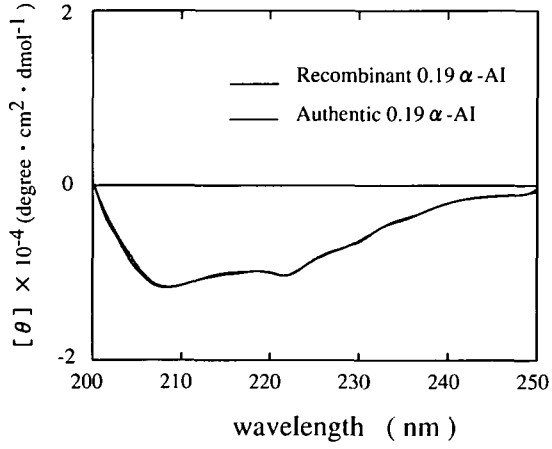

Fig. 7. **Far-UV CD spectra of recombinant and authentic 0.19 α-AI.** Far-UV CD spectra of both 0.19 α-AIs were measured as described under "MATERIALS AND METHODS." The solid line shows the spectrum of recombinant 0.19 α-AI and the thin line, that of authentic 0.19 α-AI.

Renaturation, Purification, and Characterization of the Recombinant α-AI—The expressed recombinant 0.19 α-AI was accumulated as insoluble form, possibly as inclusion bodies, in *E. coli*. The subunit of natural 0.19 α-AI contains five disulfide bonds, so a refolding step was required to acquire full inhibitory activity with correct disulfide bridges. The result of SDS-PAGE in the presence and absence of a reducing reagent indicated that the inhibitor was accumulated as the reduced form in *E. coli* (data not shown). Hence, the *E. coli* cells (2-4 g/liter LB broth) were sonicated and the insoluble fraction was solubilized by incubation with 8.0 M urea in 10 mM Tris-HCl, pH 8.0 for 30 min at 37°C. Then, the renaturation of the denatured protein was carried out by successive dialysis (two steps) as described in "MATERIALS AND METHODS" (*39*). The resulting renatured inhibitor was purified by two steps of anion exchange chromatography. Native-PAGE showed that the mobility (R_f=0.19) of the purified recombinant material (10-20 mg obtained) was identical with that of the authentic sample (data not shown here). Also, the amino acid sequence analysis revealed that the N-terminal 13 residues were identical with those of the authentic sample, indicating the removal of *N*-formylmethionine, and the peptide mappings of the two α-AIs showed almost identical patterns (Fig. 6). In addition, the conformations of the recombinant and authentic materials were estimated from their far-UV CD spectra, which showed very similar profiles with double troughs near 206 and 222 nm, suggesting an α-helix-dominant protein (Fig. 7). In the process of removing the denaturant at alkaline pH, free sulfhydryl groups were oxidized by oxygen in air to form the appropriate S-S linkages spontaneously, and the renatured inhibitor

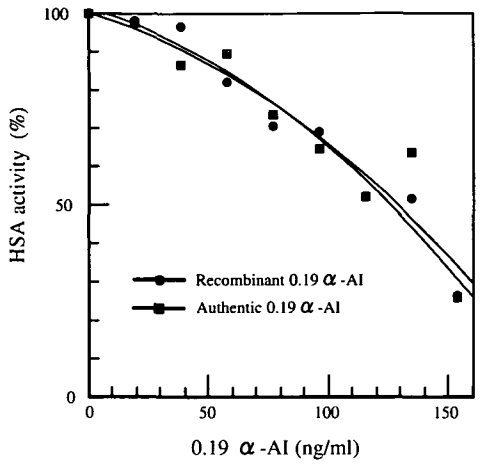

Fig. 8. **Inhibitory activity of recombinant and authentic 0.19 α-AI.** The inhibitory activity of both 0.19 α-AIs towards human salivary α-amylase was measured as described under "MATERIALS AND METHODS." —●—: recombinant 0.19 α-AI. —■—: authentic 0.19 α-AI.

recovered its inhibitory activity. In the renaturation procedure, a low protein concentation was very important since high protein concentration led to the formation of aggregates of insoluble, inactive protein. The inhibitory activity of the recombinant 0.19 α-AI for human salivary α-amylase (HSA) was measured and the result showed that the recombinant 0.19 α-AI had the same degree of inhibitory activity as the authentic product (Fig. 8).

The results of N-terminal amino acid sequencing, peptide mapping and CD spectroscopy of the gene product were identical with those of the authentic 0.19 α-AI. It also exhibited almost the same inhibitory activity as the authentic material towards salivary amylase. Therefore, in summary, we have succeeded in establishing an overexpression-preparation system for the active recombinant inhibitor. However, it is necessary to examine the assignment of disulfide bonds in both recombinant and authentic α-AI. We have investigated this problem and the results will be presented elsewhere.

Recently the three-dimensional structure of the bifunctional amylase/trypsin inhibitor from ragi seed (RBI) was determined (*20*). The RBI shows 26% amino acid sequence homology with 0.19 α-AI and has ten Cys residues forming five disulfide bonds at very similar positions to those of 0.19 α-AI. Thus, some conformational information is now available. Additionally, the crystallization of 0.19 α-AI was reported (*40*) and the elucidation of its whole three-dimensional structure is therefore feasible. The specific inhibitory mechanism of α-AI from plants has not been established, but our overexpression-preparation system will enable us to study the inhibitory mechanism by genetic modification and also structural-biological techniques.

REFERENCES

1. Aschauer, H., Vértesy, L., and Braunitzer, G. (1981) The sequence of the α-amylase inhibitor Hoe-467A (α-amylase inactivator Hoe-467A) from *Streptomyces tendae* 4158. *Hoppe-Seyler's Z. Physiol. Chem.* **362**, 465-467
2. Murai, H., Hara, S., Ikenaka, T., Goto, A., Arai, M., and Murao, S. (1985) Amino acid sequence of protein α-amylase inhibitor from *Streptomyces griseosporeus* YM-25. *J. Biochem.* **97**, 1129-1133
3. Hirayama, K., Takahashi, R., Akashi, S., Fukuhara, K., Oouchi, N., Murai, A., Arai, M., Murao, S., Tanaka, K., and Nojima, I. (1987) Primary structure of Paim I, an α-amylase inhibitor from *Streptomyces corchorushii*, determined by the combination of Edman degradation and fast atom bombardment mass spectrometry. *Biochemistry* **26**, 6483-6488
4. Vértesy, L. and Tripier, D. (1985) Isolation and structure elucidation of an α-amylase inhibitor, AI-3688, from *Streptomyces aureofaciens*. *FEBS Lett.* **185**, 187-190
5. Hofmann, O., Vertésy, L., and Braunitzer, G. (1985) The primary structure of α-amylase inhibitor Z-2685 from *Streptomyces parvullus* FH-1641. *Biol. Chem. Hoppe-Seyler* **366**, 1161-1168
6. Arai, M., Nishimura, T., Tsukao, K., Kawaguchi, T., Hayashi, H., Shimizu, Y., and Murao, S. (1989) New proteinaceous α-amylase inhibitor (T-76) from *Streptomyces nitrosporeus*. *J. Ferment. Bioeng.* **68**, 56-57
7. Katsuyama, K., Iwata, N., and Shimazu, A. (1992) Purification and primary structure of proteinous α-amylase inhibitor from *Streptomyces chartreusis*. *Biosci. Biotech. Biochem.* **56**, 1949-1954
8. Kline, A.D., Braun, W., and Wüthrich, K. (1986) Studies by ^{1}H nuclear magnetic resonance and distance geometry of the solution conformation of the α-amylase inhibitor Tendamistat. *J. Mol. Biol.* **189**, 377-382
9. Pflugrath, J. W., Wiegand, G., Huber, R., and Vértesy, L. (1986) Crystal structure determination, refinement and the molecular model of the α-amylase inhibitor Hoe-467A. *J. Mol. Biol.* **189**, 383-386
10. Yoshida, M., Nakai, T., Fukuhara, K., Saitoh, S., Yoshikawa, W., Kobayashi, Y., and Nakamura, H. (1990) Three-dimensional structure of an α-amylase inhibitor HAIM as determined by nuclear magnetic resonance methods. *J. Biochem.* **108**, 158-165
11. O'Connell, J.F., Bender, R., Engels, J.W., Koller, K.P., Scharf, M., and Wüthrich, K. (1994) The nuclear-magnetic-resonance solution structure of the mutant α-amylase inhibitor [R19L] Tendamistat and comparison with wild-type Tendamistat. *Eur. J. Biochem.* **220**, 763-770
12. Wiegand, G., Epp, O., and Huber, R. (1995) The crystal structure of porcine pancreatic α-amylase in complex with the microbial inhibitor Tendamistat. *J. Mol. Biol.* **247**, 99-110
13. Weselake, R.J., MacGregor, A.W., and Hill, R.D. (1983) An endogenous α-amylase inhibitor in barley kernels. *Plant Physiol.* **72**, 809-812
14. Lyons, A., Richardson, M., Tatham, A.S., and Shewry, P.R. (1987) Characterization of homologous inhibitors of trypsin and α-amylase from seeds of rye. *Biochim. Biophys. Acta* **915**, 305-313
15. Powers, J.R. and Whitaker, J.R. (1977) Purification and characterization of an α-amylase inhibitor from red kidney bean (*Phaseolus vulgaris*). *J. Food. Biochem.* **1**, 239-260
16. Campos, F.A.P. and Richardson, M. (1983) The complete amino acid sequence of the bifunctional α-amylase/trypsin inhibitor from seeds of ragi (Indian finger millet, *Eleusine coracana* Gaertneri.). *FEBS Lett.* **152**, 300-304
17. Chagolla, L.A., Blanco, L.A., Patthy, A., Sánchez, R., and Pongor, S. (1994) A novel α-amylase inhibitor from amaranth (*Amaranthus hypocondriacus*) seeds. *J. Biol. Chem.* **269**, 23675-23680
18. Suzuki, K., Ishimoto, M., and Kitamura, K. (1994) cDNA sequence and deduced primary structure of an α-amylase inhibitor from a bruchid-resistant wild common bean. *Biochim. Biophys. Acta* **1206**, 289-291
19. Zemke, K.J., Müller, F.A., Jany, K.D., Pal, G.P., and Saenger, W. (1991) The three-dimensional structure of the bifunctional proteinase K/α-amylase inhibitor from wheat (PKI3) at 2.5 Å resolution. *FEBS Lett.* **279**, 240-242
20. Strobl, S., Mühlhahn, P., Bernstein, R., Wiltscheck, R., Maskos, K., Wunderlich, M., Huber, R., Glockshuber, R., and Holak, T.A.

(1995) Determination of the three-dimensional structure of the bifunctional α-amylase/trypsin inhibitor from ragi seeds by NMR spectroscopy. *Biochemistry* **34**, 8281-8293
21. Deponte, R., Parlamenti, R., Petrucci, T., Silano, V., and Tomassi, M. (1976) Albumin α-amylase inhibitor families from wheat flour. *Cereal Chem.* **53**, 805-819
22. Maeda, K., Wakabayashi, S., and Matsubara, H. (1985) Complete amino acid sequence of an α-amylase inhibitor in wheat kernel (0.19-inhibitor). *Biochim. Biophys. Acta* **828**, 213-221
23. Kashlan, N. and Richardson, M. (1981) The complete amino acid sequence of a major wheat protein inhibitor of α-amylase. *Phytochemistry* **20**, 1781-1784
24. Maeda, K., Hase, T., and Matsubara, H. (1983) Complete amino acid sequence of an α-amylase inhibitor in wheat kernel. *Biochim. Biophys. Acta* **743**, 52-57
25. Buonocore, V., Gramenzi, F., Pace, W., Petrucci, T., Poerio, E., and Silano, V. (1980) Interaction of wheat monomeric and dimeric protein inhibitors with α-amylase from yellow mealworm (*Tenebrio molitor* L.) larva. *Biochem. J.* **187**, 637-645
26. Buonocore, V., Giardina, P., Parlamenti, R., Poerio, E., and Silano, V. (1984) Characterisation of chicken pancreas α-amylase isozymes and interaction with protein inhibitors from wheat kernel. *J. Sci. Food Agric.* **35**, 225-232
27. García, M.F., Carbonero, P., and García, O.F. (1991) Site-directed mutagenesis and expression in *Escherichia coli* of WMAI-1, a wheat monomeric inhibitor of insect α-amylase. *Plant Mol. Biol.* **17**, 1005-1011
28. Takase, K. (1994) Site-directed mutagenesis reveals critical importance of the catalytic site in the binding of α-amylase by wheat proteinaceous inhibitor. *Biochemistry* **33**, 7925-7930
29. Sanchez, M.R., Barber, D., Mendez, E., García, O.F., and Salcedo, G. (1986) Genes encoding α-amylase inhibitors are located in the short arms of chromosomes 3B, 3D, and 6D of wheat (*Triticum aestivum* L.). *Theor. Appl. Genet.* **72**, 108-113
30. O'Connor, C.M. and McGeeney, K.F. (1981) Isolation and characterization of four inhibitors from wheat flour which display differential inhibition specificities for human salivary and human pancreatic α-amylases. *Biochim. Biophys. Acta* **658**, 387-396
31. Laemmli, U.K. (1970) Cleavage of structural proteins during the assembly of the head of bacteriophage T4. *Nature* **227**, 680-685
32. Zuker, M. and Stiegler, P. (1981) Optimal computer folding of large RNA sequences using thermodynamics and auxiliary information. *Nucleic Acids Res.* **9**, 133-148
33. Kaji, H., Samejima, T., Kumagai, I., Hibino, T., Miura, K., and Takeda, A. (1990) Efficient preparation of human recombinant cystatin A by *Escherichia coli*. *Biol. Chem. Hoppe-Seyler* **371**, Suppl., 145-150
34. Sanger, F., Nicklen, S., and Coulson, A.R. (1977) DNA sequencing with chain-terminating inhibitors. *Proc. Natl. Acad. Sci. USA* **74**, 5463-5467
35. Lodish, H.F. (1970) Secondary structure of bacteriophage f2 ribonucleic acid and the initiation of *in vitro* protein biosynthesis. *J. Mol. Biol.* **50**, 689-702
36. Steege, D.A. (1977) 5′-Terminal nucleotide sequence of *Escherichia coli* lactose repressor mRNA: Features of translational initiation and reinitiation sites. *Proc. Natl. Acad. Sci. USA* **74**, 4163-4167
37. Hall, M.N., Gabay, J., Débarbouillé, M., and Schwartz, M. (1982) A role for mRNA secondary structure in the control of translation initiation. *Nature* **295**, 616-618
38. Schoner, B.E., Belagaje, R.M., and Schoner, R.G. (1986) Translation of a synthetic two-cistron mRNA in *Escherichia coli*. *Proc. Natl. Acad. Sci. USA* **83**, 8506-8510
39. Kawaguchi, Y., Shimizu, N., Nishimori, K., Uozumi, T., and Beppu, T. (1984) Renaturation and activation of calf prochymosin produced in an insoluble form in *Escherichia coli*. *J. Biotechnol.* **1**, 307-315
40. Miyazaki, T., Morimoto, T., Fukuyama, K., and Matsubara, H. (1994) Crystallization and preliminary X-ray diffraction studies of the α-amylase inhibitor coded 0.19 from wheat kernel. *J. Biochem.* **115**, 179-181